

CSF1/CSF1R-mediated Crosstalk Between Choroidal Vascular Endothelial Cells and Macrophages Promotes Choroidal Neovascularization

Yamei Zhou,¹ Jia Zeng,¹ Yuanyuan Tu,² Lele Li,³ Shu Du,² Linling Zhu,² Xiaomin Cang,⁴ Jiajie Lu,⁵ Manhui Zhu,² and Xiaojuan Liu¹

¹Department of Pathogen Biology, Medical College, Nantong University, Nantong, Jiangsu, China

²Department of Ophthalmology, Lixiang Eye Hospital of Soochow University, Suzhou, Jiangsu, China

³Department of Ophthalmology, the Second Affiliated Hospital of Nantong University, Nantong, Jiangsu, China

⁴Department of Endocrinology, the Second Affiliated Hospital of Nantong University, Nantong, Jiangsu, China

⁵Medical College, Nantong University, Nantong, Jiangsu, China

Correspondence: Manhui Zhu, Department of Ophthalmology, Lixiang Eye Hospital of Soochow University, 200 Ganjiang East Road, Suzhou, Jiangsu, 21500, China; zhumanhuiye@126.com.

Xiaojuan Liu, Department of Pathogen Biology, Medical College, Nantong University, No. 19, Qixiu Road, Nantong, Jiangsu, 226001, China; lxj@ntu.edu.cn.

YZ, JZ, MZ, and XL contributed equally to this study.

Received: December 16, 2020

Accepted: March 4, 2021

Published: March 25, 2021

Citation: Zhou Y, Zeng J, Tu Y, et al. CSF1/CSF1R-mediated crosstalk between choroidal vascular endothelial cells and macrophages promotes choroidal neovascularization. *Invest Ophthalmol Vis Sci.* 2021;62(3):37. <https://doi.org/10.1167/iovs.62.3.37>

PURPOSE. This study examined the role of the CSF1/CSF1R axis in the crosstalk between choroidal vascular endothelial cells (CVECs) and macrophages during the formation of choroidal neovascularization (CNV).

METHODS. Quantitative reverse transcriptase (qRT)-PCR, Western blot and ELISA measured the production and release of CSF1 from human choroidal vascular endothelial cells (HCVECs) under hypoxic conditions. Western blot detected CSF1 released from HCVECs under hypoxic conditions that activated the PI3K/AKT/FOXO1 axis in human macrophages via binding to CSF1R. Transwell migration assay, qRT-PCR, and Western blot detected the effect of CSF1 released from HCVECs on macrophage migration and M2 polarization via the CSF1R/PI3K/AKT/FOXO1 pathway. Incorporation of 5-ethynyl-20-deoxyuridine, transwell migration, and tube formation assays detected the effects of CSF1/CSF1R on the behaviors of HCVECs. Fundus fluorescein angiography (FFA), indocyanine green angiography (ICGA), and immunofluorescence detected the effect of blockade of CSF1/CSF1R on mouse laser-induced CNV. Color fundus photograph, ICGA, and FFA detected CNV lesions in neovascular AMD (nAMD) patients. ELISA detected CSF1 and CSF1R in the aqueous humor of age-related cataract and nAMD patients.

RESULTS. CSF1 released from HCVECs under hypoxic conditions activated the PI3K/AKT/FOXO1 axis in human macrophages via binding to CSF1R, promoting macrophage migration and M2 polarization via up-regulation of the CSF1R/PI3K/AKT/FOXO1 pathway. Human macrophages promoted the proliferation, migration, and tube formation of HCVECs in a CSF1/CSF1R-dependent manner under hypoxic conditions. CSF1/CSF1R blockade ameliorated the formation of mouse laser-induced CNV. CSF1 and CSF1R were increased in the aqueous humor of nAMD patients.

CONCLUSIONS. Our results affirmed the crucial role of CSF1/CSF1R in boosting the formation of CNV and offered potential molecular targets for the treatment of nAMD.

Keywords: neovascular AMD, choroidal neovascularization, CSF1, colony stimulating factor 1 receptor (CSF1R), human choroidal vascular endothelial cells, macrophages

AMD is the leading cause of irreversible vision loss in the elderly population in developed countries. AMD is divided into two subtypes: neovascular and nonneovascular. Neovascular AMD (nAMD) is characterized by choroidal neovascularization (CNV), in which an abnormal neovasculature results in intraretinal and subretinal hemorrhage and macular edema, which ultimately results in severe subretinal fibrosis with complete vision loss. The leading treatment for CNV is intravitreal injection of antivascular VEGF (also known as VEGF-A), which principally targets vascular endothelial cells (ECs). However, tolerance is modest, and drug resistance frequently occurs

for most patients within the first four years of treatment,¹ which indicates the existence of other vital proangiogenic elements. Previous studies revealed that infiltrating macrophages, which are the predominant population of immune cells, played an essential role in the pathogenesis of CNV. M1 macrophages with specific markers, such as inducible nitric oxide synthase (iNOS), IL-6, and TNF- α , inhibit angiogenesis.² M2 macrophages with specific markers, including arginase-1 (Arg1), mannose receptor C type 1 (CD206), and cluster of differentiation 163 (CD163), also promote pathological angiogenesis during CNV.³ Nakamura and colleagues⁴ provide evidence that increased IL-10 in

senescent mouse eyes activates signal transducer and activator of transcription 3 signaling, which induced the alternative activation of macrophages and vascular proliferation. Tissue factor is primarily derived from infiltrating M2 macrophages and induces CNV.^{5,6} Therefore macrophage polarization may be a target for the treatment of CNV.

Colony-stimulating factor 1 (CSF1), which is also known as macrophage-CSF, up-regulates macrophage recruitment⁷ and M2-type polarization.⁸ Transcripts encoding CSF-1 are downregulated in bovine retinal endothelial cells compared to choroidal endothelial cells under hypoxic conditions.⁹ CSF1 binds to colony stimulating factor 1 receptor (CSF1R) to activate downstream signaling pathways. For example, CSF1 promotes macrophage survival via activation of the phosphoinositide 3-kinase (PI3K)/protein kinase B (AKT) pathway.¹⁰ The transcription factor fork head box protein O1 (FOXO1) facilitates M2-like macrophage activation in allergic asthma.¹¹ The PI3K/AKT/FOXO1 pathway also boosts macrophage M2-like polarization.¹² On the basis of previous studies, we hypothesized that choroidal vascular endothelial cells would release CSF1 during hypoxic condition, bind to CSF1R on infiltrating macrophages, and activate the PI3K/AKT/FOXO1 pathway to enhance macrophage M2 polarization.

The present study investigated the role of CSF1/CSF1R in the crosstalk between CVECs and macrophages during CNV. Our results further clarified the crucial effect of innate immunity on the pathogenesis of CNV.

MATERIALS AND METHODS

Cell Culture and Treatments

Human choroidal vascular endothelial cells (HCVECs; CP-H092, Procell, China) and human peripheral blood monocyte-derived macrophages¹³ were cultured in Dulbecco's modified Eagle's medium (113-24-6; Millipore, Burlington, MA, USA) with 10% fetal bovine serum (FBS; F8687; Merck, Kenilworth, NJ, USA), and 1% penicillin-streptomycin (516106; Millipore).

HCVECs were divided into normal (normoxia; 95% O₂ and 5% CO₂) and hypoxia groups (1% O₂, 94% N₂, and 5% CO₂) in a gas-controlled incubator (Forma 2; ThermoFisher Scientific, Waltham, MA, USA). Macrophages were divided into the following treatment conditions: normal control (normoxia); human CSF1 recombinant protein (216-MC; R&D Systems, Minneapolis, MN, USA); human CSF1 recombinant protein + pexidartinib (PLX3397; CSF1R inhibitor; S7818; Selleck Chemicals, Houston, TX, USA; 10 μM for 24 hours); coculture with HCVECs under normoxia; coculture with HCVECs under hypoxia; coculture with HCVECs under hypoxia + CSF1 neutralizing antibody (MAB216; R&D Systems; 0.2 μg/mL for 24 hours); coculture with HCVECs under hypoxia + PLX3397; coculture with HCVECs under hypoxia + LY294002 (PI3K/AKT inhibitor; S1105; Selleck Chemicals; 10 μM for 24 hours); and coculture with HCVECs under hypoxia + AS1842856 (FOXO1 inhibitor; S8222; Selleck Chemicals; 0.1 μM for 24 hours).

Real-Time RT-PCR

Total RNA was extracted from HCVECs or macrophages using Tri Reagent (93289; Sigma-Aldrich Corp., St. Louis, MO, USA). First-strand cDNA was synthesized using the

High Capacity cDNA Reverse Transcription Kit (4368814; Applied Biosystems, Foster City, CA, USA) and an RNase inhibitor (AM2694; Invitrogen, Carlsbad, CA, USA). The mRNA levels of the genes were quantified using real-time RT-PCR (qRT-PCR) and the Platinum Syber Green QAPCR Super Mix-UDG w/ROX kit (11744100; Invitrogen). The $2^{-\Delta\Delta Ct}$ formula was used to quantify the relative expression of the genes, which were normalized to glyceraldehyde-3-phosphate dehydrogenase (GAPDH). The following forward and reverse sequences of primers used for qRT-PCR were used: CSF1 (NM_000757.6) 5'-AAAGTTTGCTGGGTCCTCT-3' and 5'-TCCTCGGTGATACTCCTGCT-3'; iNOS (NM_000625.4) 5'-CCTCCCATCCTTGATCCTC-3' and 5'-CCAAACACCAAGGTCATGCG-3'; Arg1 (NM_000045.4) 5'-ACTTAAAGAACAAGAGTGTGATGTG-3' and 5'-CATGGCCAGAGATGCTTCCA-3'; and GAPDH (NM_001289745.3) 5'-GACAGTCAGCCGCATCTTCT-3' and 5'-GCGCCCAATACGACCAAATC-3'.

Western Blot

Lysates of HCVECs, macrophages, and mouse retina-retinal pigment epithelium (RPE)-choroidal tissues were separated using sodium dodecyl sulfate-polyacrylamide gel electrophoresis (SDS-PAGE) followed by transfer onto polyvinylidene fluoride membranes. The membranes were blocked in Tris-buffered saline solution with 0.5% Tween 20 containing 5% BSA and probed with primary antibodies overnight at 4°C. The membranes were washed three times and incubated with secondary antibodies. The primary antibodies used in the study included anti-CSF1 (14779-1-AP; Proteintech, Rosemont, IL, USA), p-CSF1R (Y723; 3155), CSF1R (3152), p-PI3K (Y458 and Y199; PA5-17387; Invitrogen), PI3K (MA1-74183; Invitrogen), p-AKT (S473; 4060), AKT (4691), p-FOXO1 (S256; 84192), FOXO1 (2880), iNOS(18985-1-AP; Proteintech), Arg1 (16001-1-AP; Proteintech), β-actin (4967), and GAPDH (2118). The secondary antibodies included horseradish peroxidase-linked horse anti-mouse IgG (7076) and goat anti-rabbit IgG (7074). Antibodies with unmentioned suppliers were purchased from Cell Signaling Technology (Danvers, MA, USA). Immunoreactivity was visualized using enhanced chemiluminescence (32106; ThermoFisher Scientific).

ELISA

For the measurement of cell culture supernatants, HCVECs (1 × 10⁶ cells per well) were seeded in a 48-well plate. The supernatants were collected from the cell cultures before the cells were harvested. The CSF1 levels in the cell culture supernatant were measured using a human CSF1 ELISA kit (EHCSF1; Invitrogen; assay range, 2.78–2000 pg/mL). The quantities in whole cell lysates were measured after cell harvest. For the detection of VEGF in mouse retina-RPE-choroid tissues, a mouse VEGF ELISA kit (MMV00; R&D Systems; assay range, 7.8–500 pg/ml) was used. For the measurement of CSF1 and p-CSF1R (Y723) levels in the aqueous humor (AH) from age-related cataract (ARC) and nAMD patients, the volume of AH was determined before performing ELISA. A human p-CSF1R ELISA kit (OKAG01687; Aviva Systems Biology, San Diego, CA, USA; dynamic range, >5000 cells) was used. The optical density of each well was detected immediately using a microplate reader at 450 nm.

Transwell Migration Assay

The upper chamber was inoculated with 2×10^6 HCVECs or macrophages in FBS-free medium cultured under different conditions for 24 hours. The lower chamber was filled with medium containing 10% FBS as a chemotaxis force. The chambers were fixed for 20 minutes, and 500 μ L 0.1% crystal violet was added for 10 minutes before washing. After 24 hours, cells in the upper chamber were removed with cotton swabs, and cells on the underside were fixed with 4% paraformaldehyde for 10 minutes at room temperature. After washing and air drying, stained cells in four randomly selected fields were photographed and counted under a light microscope (Olympus, Tokyo, Japan; magnification $\times 100$).

5-Ethynyl-20-Deoxyuridine Assay

A 5-Ethynyl-20-deoxyuridine (EdU) assay kit with Alexa Fluor 594 dye (17-10527; Millipore) was used to detect the proliferation of HCVECs. HCVECs were seeded into confocal plates at a density of 1×10^6 cells per well. HCVECs were incubated with 50 μ M EdU buffer at 37°C for two hours, fixed with 4% paraformaldehyde for 0.5 hour and permeabilized with 0.1% Triton X-100 for 20 minutes. The EdU solution was added to the culture, and nuclei were stained with 4',6-diamidino-2-phenylindole (D1306; Invitrogen). The results were visualized under a fluorescence microscope (Olympus). The excitation wavelength was 584 nm, and the emission wavelength was 603 nm.

Tube Formation Assay

A 24-well plate was polymerized with growth factor-reduced Matrigel (356230; BD Biosciences, Franklin Lakes, NJ, USA) for 30 minutes at 37°C. HCVECs (2×10^4) were incubated under different conditions for 24 hours before image acquisition. The capillary tubes were quantified under a bright-field microscope at magnification $\times 100$, and the total lengths of the completed tubule structures were measured.

Mouse Laser-Induced CNV Model and Treatments

C57BL/6J male mice aged six to eight weeks were purchased from the Animal Experimental Center of Nantong University. All procedures and animal care were performed in accordance with the guidelines of the Association for Research in Vision and Ophthalmology on the use of animals in research and were approved by the Animal Ethical Committee at Nantong University. For CNV induction, the mice were anesthetized via an intraperitoneal injection of Zoletil 50 (Virbac, Carros, France) and Rompun (Bayer Healthcare, Leverkusen, Germany). A mixture of 0.5% tropicamide and 5% phenylephrine (Mydracyl; Wilson Ophthalmic Corporation, Mustang, OK, USA) was instilled for pupil dilation. Laser photocoagulation (spot diameter 200 μ m, duration 20 ms, power 120 mW, four spots/eye) was performed using a PASCAL diode ophthalmic laser system (neodymium-doped yttrium aluminum garnet [Nd:YAG], 532 nm; Topcon Medical Laser Systems, Livermore, CA, USA), and laser burns were produced in the 3, 6, 9, and 12 o'clock positions around the optic disc with the laser focused on the RPE. The presence of a bubble confirmed the disruption of Bruch's membrane. The mice were divided into normal, CNV 7 d, CNV 7 d +

PBS (vehicle control), CNV 7 d + PLX3397 (intraperitoneal injection, 40 mg/kg on day 1), and CNV 7 d + conbercept (Chengdu Kanghong Biotechnologies Co., Chengdu, China; intravitreal injection, 1 μ L of 10 mg/mL on day 1) groups, with 16 mice in each group. Three mice were excluded from the experiments because of hemorrhage at the site of laser administration.

Fundus Angiography

To determine CNV leakage and area, fundus fluorescein angiography and indocyanine green angiography (ICGA) in mice were performed seven days after CNV. The mice were anesthetized, and pupils were dilated. Mice were intraperitoneally injected with fluorescein AK-FLUOR (17478025310; Akorn Pharmaceuticals, Decatur, IL, USA) at 5 μ g/g body weight and indocyanine green (1340009; Merck) at 0.075 μ g/g body weight. Fluorescent fundus images were acquired 5 min and 10 min after fluorescein injection using a retinal imaging microscope (Micron IV; Phoenix Research Laboratories, Pleasanton, CA, USA). Two independent blinded observers graded fluorescein leakage using previously established criteria.¹⁴ Briefly, Grade 0 lesions had no hyperfluorescence, Grade 1 lesions had hyperfluorescence with negligible leakage, Grade 2a lesions had low levels of leakage within the lesion area, and Grade 2b lesions had high levels of leakage outside the area of the lesion. The total CNV area was quantified in ICGA images using ImageJ software.

Immunohistochemistry on Choroidal Flat-Mounts

Seven days after CNV, the cornea and crystalline lens were removed from the enucleated eye, followed by a radial relaxing incision in the eye cup of the choroid and sclera for immunostaining on choroidal flat mounts. The choroidal tissue specimens were incubated with Alexa Fluor 488-conjugated isolectin-B4 (IB4) (I21411; ThermoFisher Scientific) and Alexa Fluor 568-conjugated CD31 (bs-0468R-A594; Bioss Antibodies Inc., Woburn, MA, USA) antibodies prepared in immunocytochemistry buffer at 4°C for 24 hours.

Patient Subjects

The Institutional Review Board of Lixiang Eye Hospital of Soochow University approved this study (approval number: SLER2020125). Ten patients with nAMD who received no therapy were recruited, and 10 age-matched patients with ARCs who underwent routine phacoemulsification surgery served as controls. Informed consent was obtained from all nAMD and ARC patients. The following exclusion criteria were used: (1) age younger than 60 years; (2) history of ocular diseases other than ARC; (3) any previous intraocular surgery, verteporfin photodynamic therapy, or intravitreal triamcinolone injection; (4) previous history of any intravitreal anti-VEGF treatment within the last six months in the study eye or within the last three months in the fellow eye; (5) amblyopia; (6) cataract of grade >3 according to the Emery-Little nuclear hardness classification¹⁵; and (7) Alzheimer's disease or other types of dementia.

Detailed information on the subjects is shown in the Table. Age, sex, medical history, and ocular history were assessed at the initial visit for each patient, and BCVA

TABLE. Clinical Profile of nAMD and ARC Patients Participating in the Study was Shown

	nAMD Patients	ARC Patients	P Value
Eyes, n	10	10	—
Age, years	77.2 ± 3.8	78.4 ± 3.2	0.642
Females/males	5/5	6/4	0.548
logMAR visual acuity	0.41 ± 0.17	0.27 ± 0.13	0.546
Systemic diseases, n(%)			
Hypertension	4 (40)	5 (50)	0.548
Diabetes	2 (20)	3 (30)	0.334
Hyperlipidemia	4 (40)	3 (30)	0.398
Coronary heart disease	1 (10)	2 (20)	0.232
Renal disease	0	0	—
Liver disease	0	0	—
Cerebrovascular disease	2 (20)	1 (10)	0.232
Alcohol intake	4 (40)	3 (30)	0.398
Smoking	2 (20)	4 (40)	0.081
Ocular diseases, n (%)			
Polypoidal choroidal vasculopathy	0	0	—
Retinal angiomatous proliferation	0	0	—

nAMD, neovascular AMD; ARC, age-related cataract.

was recorded as the logMAR equivalent using a standardized Landolt visual acuity chart. Each patient also underwent color fundus photography and fluorescein angiography. The diagnosis of hypertension, coronary artery disease, or diabetes was based on data from the medical records.

Hypertension was defined as a blood pressure >140/90 mm Hg or current use of antihypertensive therapy, and diabetes was diagnosed according to information from the subjects or the use of antidiabetic medications.

Aqueous Humor Collection

All aqueous humor sample collections were performed using a standard sterilization procedure. Undiluted aqueous humor samples (200 µL from one eye) were obtained from 10 eyes of 10 nAMD patients via anterior chamber paracentesis before intravitreal ranibizumab injections and from 10 control eyes immediately before cataract surgery. Paracentesis was performed before any conjunctival or intraocular manipulation to avoid breakdown of the blood-aqueous barrier associated with surgical injury. Samples were snap-frozen and stored at -80°C until analysis.

Statistical Analysis

Data are presented as the means ± SEM. Statistical evaluations were performed using one-way ANOVA followed by Bonferroni's post hoc test. $P < 0.05$ was considered statistically significant. Analyses were performed using the statistical software SPSS 15.0.

RESULTS

Human Choroidal Vascular Endothelial Cells Produce and Release CSF1 Under Hypoxic Conditions

We first measured the production and release of CSF1 from HCVECs under hypoxic conditions. Hypoxia increased CSF1 mRNA (Fig. 1A) and protein (Figs. 1B, 1C) levels compared to normoxic conditions. Hypoxia also induced CSF1 levels

in the culture supernatant of HCVECs (Fig. 1D). These data suggest that hypoxia induces the production and release of CSF1 from HCVECs.

CSF1 Released From Human Choroidal Vascular Endothelial Cells Under Hypoxic Conditions Activates the PI3K/AKT/FOXO1 Axis in Human Macrophages Via Binding to CSF1R

CSF1 leads to CSF1R autophosphorylation and activation in malignant T cells. CSF1R signaling is associated with significant changes in gene expression and the phosphoproteome,

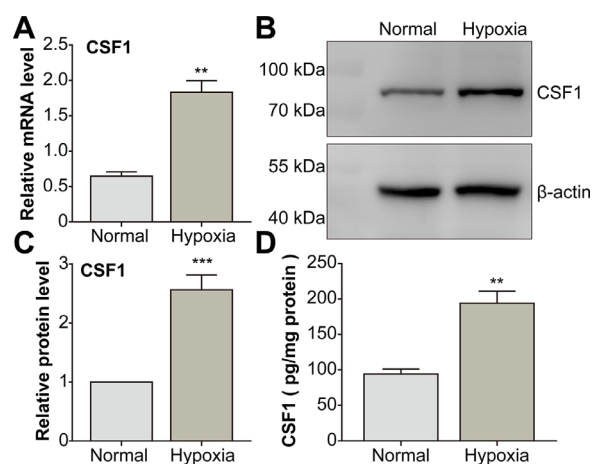


FIGURE 1. Human choroidal vascular endothelial cells (HCVECs) produce and release CSF1 under hypoxic conditions. (A) qRT-PCR was performed HCVECs were divided into normal (95% O₂, 5% CO₂) and hypoxia groups (1% O₂, 94% N₂, 5% CO₂). qRT-PCR was performed to measure CSF1 mRNA levels in HCVECs. ** $P < 0.01$, hypoxia group versus normal group. (B) Western blotting was performed to measure CSF1 protein levels. (C) The relative protein level of CSF1 was analyzed. *** $P < 0.005$, hypoxia group versus normal group. (D) ELISA was performed to measure CSF1 protein levels in the culture supernatants of HCVECs. ** $P < 0.01$, hypoxia group versus normal group. n = 5/each group.

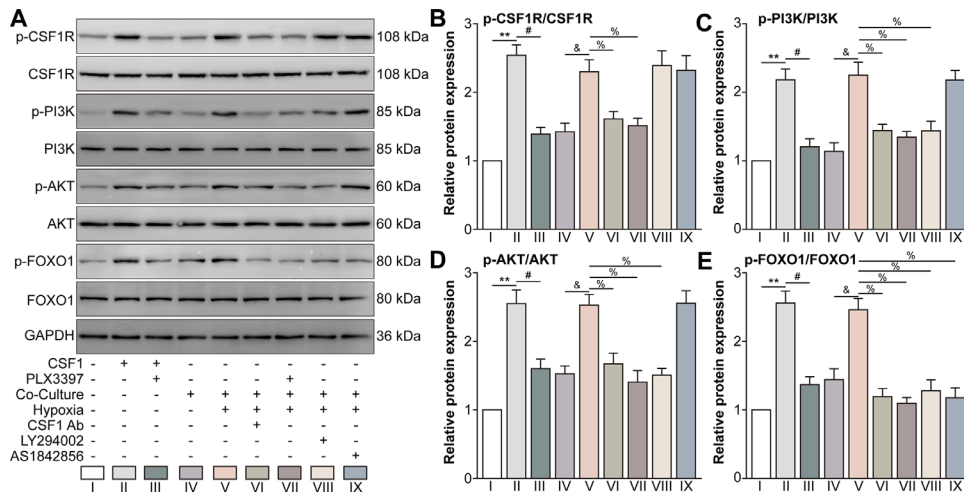


FIGURE 2. CSF1 released from human choroidal vascular endothelial cells under hypoxic conditions activates the PI3K/AKT/FOXO1 axis in human macrophages via binding to CSF1R. Human peripheral blood monocyte-derived macrophages were divided into normal control (without any treatments), human CSF1 recombinant protein, human CSF1 recombinant protein + pexidartinib (PLX3397; CSF1R inhibitor; 10 μ M for 24 hours), coculture with HCVECs under normal conditions (normoxia), coculture with human choroidal vascular endothelial cells (HCVECs) under hypoxia, coculture with HCVECs under hypoxia + CSF1 neutralizing antibody (0.2 μ g/mL for 24 hours), coculture with HCVECs under hypoxia + PLX3397, coculture with HCVECs under hypoxia + LY294002 (PI3K/AKT inhibitor; 10 μ M for 24 hours) and coculture with HCVECs under hypoxia + AS1842856 (FOXO1 inhibitor; 0.1 μ M for 24 hours) groups. **(A)** Western blot was performed to measure p-CSF1R, CSF1R, p-PI3K (Y458), PI3K, p-AKT (S473), AKT, p-FOXO1 (S256), and FOXO1 protein levels. **(B–E)** The relative protein levels of CSF1R, p-PI3K, p-AKT, and p-FOXO1 were analyzed. ** P < 0.01 versus normal group. # P < 0.05 versus CSF1 group. & P < 0.05 versus coculture under normoxia group. % P < 0.05 versus coculture under hypoxia group. n = 4/each group.

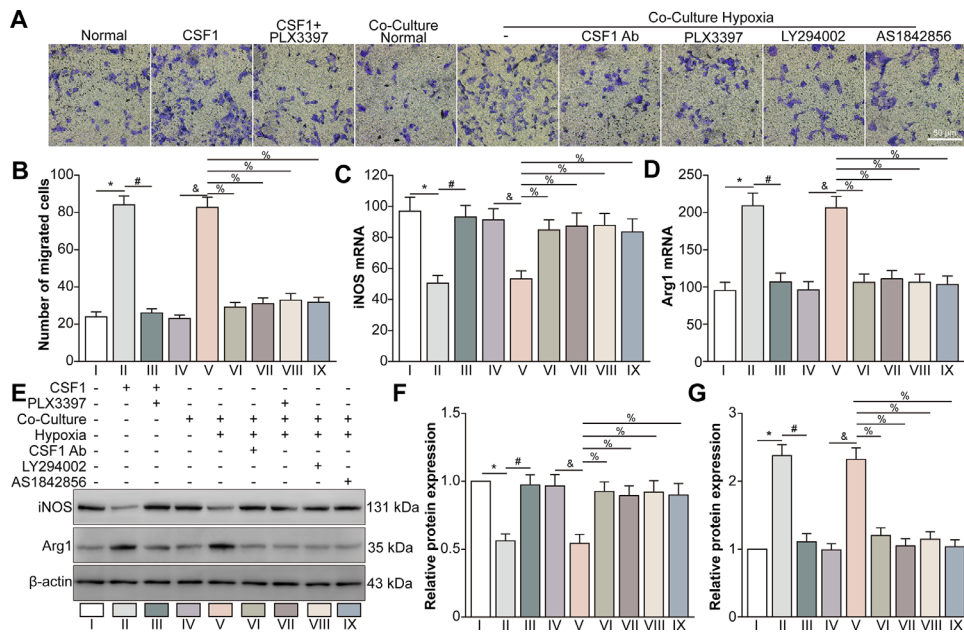


FIGURE 3. CSF1 released from human choroidal vascular endothelial cells (HCVECs) promotes macrophage migration and M2 polarization via the CSF1R/PI3K/AKT/FOXO1 pathway. Macrophages were divided into normal control, human CSF1 recombinant protein, human CSF1 recombinant protein + pexidartinib (PLX3397; CSF1R inhibitor; 10 μ M for 24 hours), coculture with HCVECs under normoxia, coculture with HCVECs under hypoxia, coculture with HCVECs under hypoxia + CSF1 neutralizing antibody (0.2 μ g/mL for 24 hours), coculture with HCVECs under hypoxia + PLX3397, coculture with HCVECs under hypoxia + LY294002 (PI3K/AKT inhibitor; 10 μ M for 24 hours), and coculture with HCVECs under hypoxia + AS1842856 (FOXO1 inhibitor; 0.1 μ M for 24 hours) groups. **(A)** Transwell assay was performed to measure macrophage migration. **(B)** The average number of migrated macrophages was analyzed. The qRT-PCR was performed to measure the mRNA levels of the M1-type macrophage marker iNOS **(C)** and the M2-type macrophage marker Arg1 **(D)**. **(E)** Western blotting was performed to measure the protein levels of iNOS and Arg1. **(F)** The relative protein levels of iNOS and Arg1 were analyzed. * P < 0.05 versus normal group. # P < 0.05 versus CSF1 group. & P < 0.05 versus coculture under normoxia group. % P < 0.05 versus coculture under hypoxia group in **Figures 3B to 3D, 3Fm and 3G**. n = 4/each group.

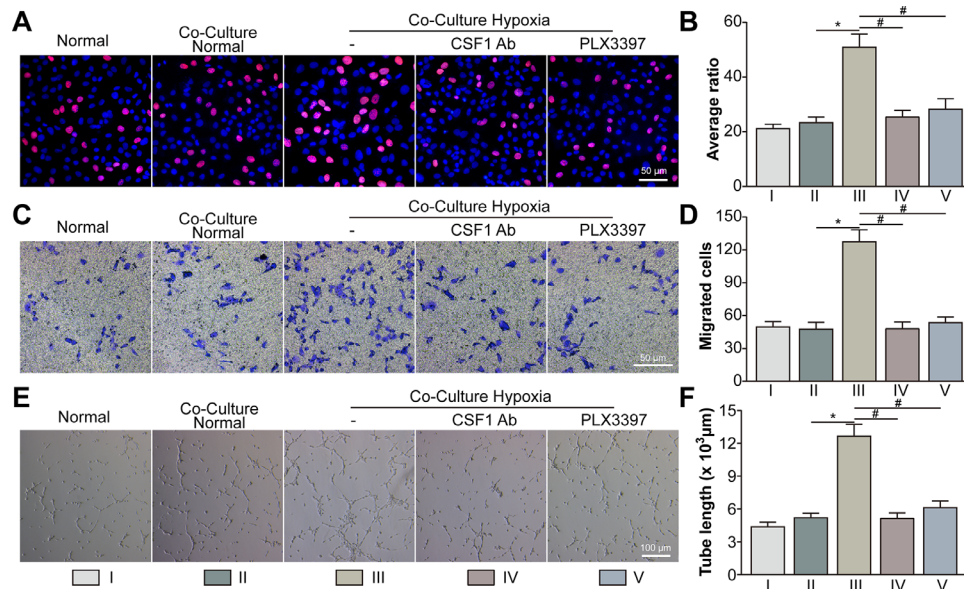


FIGURE 4. Human macrophages promote the proliferation, migration, and tube formation of human choroidal vascular endothelial cells (HCVECs) in a CSF1/CSF1R-dependent manner under hypoxic conditions. HCVECs were divided into normal control, coculture with macrophages under normoxia, coculture with macrophages under hypoxia, coculture with macrophages under hypoxia + CSF1 neutralizing antibody, and coculture with macrophages under hypoxia + PLX3397 groups. **(A)** The 5-ethynyl-20-deoxyuridine (EdU) assays were performed to measure the proliferation of HCVECs. **(B)** The average ratio of EdU-positive cells versus 4',6-diamidino-2-phenylindole-positive cells was analyzed. **(C)** Transwell assays were performed to measure the migration of HCVECs. **(D)** The average number of migrated HCVECs was analyzed. **(E)** A tube formation assay was performed to measure the tubular formation ability of HCVECs. **(F)** The total tube length was analyzed. * $P < 0.05$ versus coculture normal group. # $P < 0.05$ versus coculture hypoxia group in Figures 4B, 4D and 4F. $n = 4$ /each group.

which indicates that the PI3K/AKT/mTOR axis promotes CSF1R-mediated T-cell lymphoma growth.¹⁶ The transcription factor FOXO1 is downstream of PI3K/AKT in macrophages,¹⁷ and it facilitates M2 polarization.¹² Therefore we detected the effects of CSF1 derived from HCVECs on the PI3K/AKT/FOXO1 axis in human macrophages. P-CSF1, p-PI3K, p-AKT, and p-FOXO1 protein levels in the normal control group were low, and CSF1 administration increased these levels. The CSF1R inhibitor PLX3397 down-regulated the protein levels of p-CSF1R, p-PI3K, p-AKT, and p-FOXO1 compare to the human CSF1 recombinant protein group. When HCVECs and human macrophages were co-cultured, hypoxic conditions induced more p-CSF1R, p-PI3K, p-AKT and p-FOXO1 expression in human macrophages than normoxic conditions. A CSF1 neutralizing antibody and PLX3397 inhibited the phosphorylation of CSF1R, PI3K, AKT, and FOXO1 after coculture with HCVECs under hypoxic conditions, which indicated that CSF1 released from HCVECs bound to CSF1R to activate PI3K, AKT and FOXO1 in human macrophages. The PI3K/AKT inhibitor LY294002 inhibited the phosphorylation of PI3K, AKT, and FOXO1, with no obvious effect on the phosphorylation of CSF1R, which indicated that PI3K, AKT, and FOXO1 were downstream of CSF1/CSF1R. The FOXO1 inhibitor AS1842856 inhibited the phosphorylation of FOXO1 but showed no obvious effects on the phosphorylation of CSF1R, PI3K and AKT, which indicated that FOXO1 was downstream of CSF1R, PI3K and AKT (Fig. 2A and 2E). These data suggested that CSF1 released from HCVECs under hypoxic conditions activated the PI3K/AKT/FOXO1 axis in human macrophages via binding to CSF1R.

CSF1 Released From Human Choroidal Vascular Endothelial Cells Promotes Macrophage Migration and M2 Polarization Via the CSF1R/PI3K/AKT/FOXO1 Pathway

CSF1 promotes macrophage migration¹⁸ and M2 polarization.¹⁹ We investigated whether CSF1 affected the migration and M2 polarization of macrophages in a CSF1R/PI3K/AKT/FOXO1-dependent manner. Compared to the normal control group, human CSF1 recombinant protein enhanced the migration of macrophages, which was reversed by CSF1R inhibition. These results showed that CSF1 promoted the migration of macrophages via CSF1R. The migration of macrophages was weak HCVECs under normoxic conditions, but coculturing with HCVECs under hypoxic conditions upregulated the migration of macrophages. The CSF1 neutralizing antibodies PLX3397, LY294002 and AS1842856 inhibited the migration of macrophages under coculture hypoxic conditions, which indicated that CSF1 released from HCVECs promoted the migration of macrophages via the CSF1R/PI3K/AKT/FOXO1 pathway. CSF1 down-regulated the mRNA levels of the M1 macrophage marker iNOS, and PLX3397 reversed this effect. Coculturing with HCVECs under hypoxic conditions decreased M1-type markers compared to coculturing with HCVECs under normoxic conditions. The CSF1 neutralizing antibodies PLX3397, LY294002, and AS1842856 increased the M1-type marker iNOS (Fig. 3C), but the macrophage M2-type marker Arg1 showed the opposite tendencies (Fig. 3D). The iNOS and Arg1 protein levels showed similar tendencies as their mRNA levels (Figs. 3E, 3G). These data suggested that CSF1 released from HCVECs

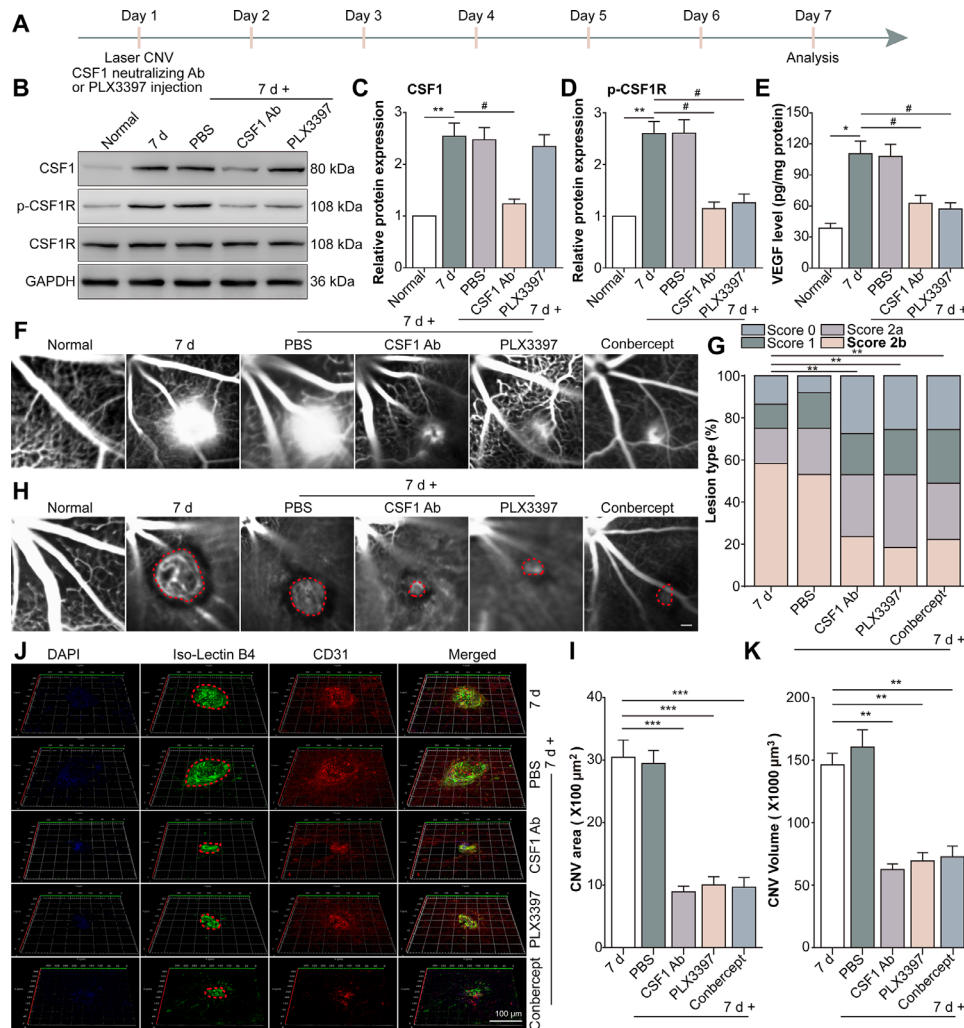


FIGURE 5. CSF1/CSF1R blockade ameliorates the formation of mouse laser-induced choroidal neovascularization (CNV). The mice were divided into normal, CNV 7 d, CNV 7 d + PBS, CNV 7 d + CSF1 neutralizing antibody, and CNV 7 d + PLX3397 groups. **(A)** The experimental process is shown. A mouse laser-induced CNV model was constructed on day 1. CSF1 neutralizing antibody or PLX3397 was injected on day 1. On day 7, the mice were sacrificed and analyzed. **(B)** Western blotting was performed to measure CSF1, p-CSF1R, and CSF1R protein levels in retina-RPE-choroid tissues. **(C, D)** The protein levels of CSF1 and p-CSF1R relative to GAPDH and CSF1R, respectively, were analyzed. $^{**}P < 0.01$ versus normal group. $^{\#}P < 0.05$ versus CNV 7 d group in Figures 5C and 5D. **(E)** The VEGF levels in mouse retina-RPE-choroid tissues were detected using ELISA. $^{*}P < 0.05$ vs. normal group. $^{\#}P < 0.05$ vs. normal group. **(F)** Fundus fluorescein angiography was performed to detect the leakage of CNV lesions. **(G)** The leakage of CNV lesions was graded. $^{**}P < 0.01$ versus CNV 7 d group. **(H)** Indocyanine green angiography was performed to detect the area of the CNV lesion. **(I)** The area of CNV lesion was analyzed. $^{***}P < 0.005$ versus CNV 7 d group. **(J)** IB4 (green), phalloidin (red), and 4',6-diamidino-2-phenylindole (blue) were labeled on mouse choroidal flat mounts. **(K)** The volume of CNV lesion was analyzed. $^{**}P < 0.01$ versus CNV 7 d group. $n = 4$ /each group.

promoted macrophage migration and M2 polarization via the CSF1R/PI3K/AKT/FOXO1 pathway.

Human Macrophages Promote the Proliferation, Migration, and Tube Formation of Human Choroidal Vascular Endothelial Cells in a CSF1/CSFR1-Dependent Manner Under Hypoxic Conditions

Previous studies demonstrated that M2-type macrophages exacerbated CNV by promoting the proliferation, migration, and tube formation of choroidal endothelial cells.²⁰ Therefore we determined the role of CSF1/CSF1R in the M2-type macrophage-regulated behaviors of HCVECs. In the normal control group, HCVECs exhibited little proliferation, migration, and tube formation. However, cocul-

turing with human macrophages under hypoxic conditions increased the proliferation, migration, and tube formation of HCVECs compared to HCVECs cocultured with human macrophages under normoxic conditions. ACSF1 neutralizing antibody and PLX3397 inhibited the behaviors of HCVECs (Figs. 4A, 4F). These results showed that macrophages promoted the proliferation, migration and tube formation of HCVECs in a CSF1/CSFR1-dependent manner under hypoxic conditions.

CSF1/CSF1R Blockade Ameliorates the Formation of Mouse Laser-Induced CNV

We further identified the effect of CSF1/CSF1R blockade on CNV. A mouse laser-induced CNV model was constructed on day 1. A CSF1 neutralizing antibody or PLX3397 was

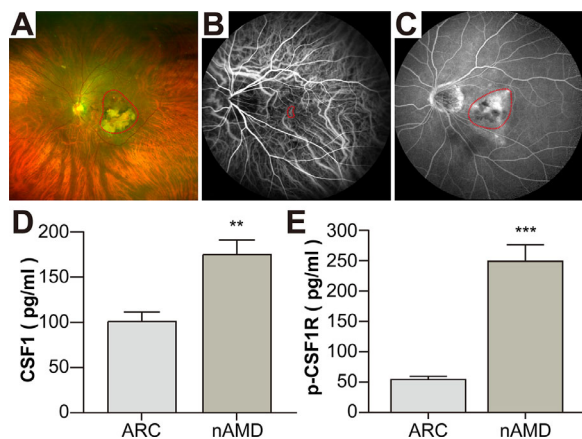


FIGURE 6. CSF1 and CSF1R are increased in the aqueous humor of neovascular AMD (nAMD) patients. (A) Color fundus photograph showing the leakage of choroidal neovascularization (CNV) in the left eye of an nAMD patient. The region around the red dotted line represents the CNV lesion. (B) Indocyanine green angiography of the left eye of an nAMD patient is shown. The region around the red dotted line represents neovascularization in early-stage nAMD. (C) Fluorescein fundus angiography of the same eye as in Figure 6B is shown. The region around the red dotted line represents vascular leakage in the late stage of nAMD. The protein levels of CSF1 (D) and CSF1R (E) in the aqueous humor of age-related cataract and nAMD patients were detected using ELISA. $n = 10$ /each group.

injected on day 1. The mice were sacrificed and analyzed on day 7 (Fig. 5A). The CSF1 neutralizing antibody reversed CNV-induced CSF1, and the CSF1 neutralizing antibody and PLX3397 reversed CNV-induced phosphorylation of CSF1R (Figs. 5B, 5D). The CSF1 neutralizing antibody and PLX3397 also decreased CNV-induced VEGF levels in retina-RPE-choroid tissues (Fig. 5E). The CSF1 neutralizing antibody and PLX3397 improved the leakage of CNV, which was indicated by the protective effect of conbercept (Figs. 5F, 5G). The CSF1 neutralizing antibody and PLX3397 also reduced the area (Figs. 5H, 5J) and volume (Figs. 5J, 5K) of CNV, which was indicated by the therapeutic roles of conbercept. These results showed that CSF1/CSF1R blockade ameliorated the formation of mouse laser-induced CNV.

CSF1 and CSF1R are Increased in the Aqueous Humor of nAMD Patients

The clinical features of the nAMD and ARC patients are listed in the Table. Among the 10 AMD patients (10 eyes),

four patients (40%) had hypertension, two patients (20%) had diabetes, four patients (40%) had hyperlipidemia, one patient (10%) had coronary heart disease, and two patients (20%) had cerebrovascular disease. Among the 10 ARC patients (10 eyes), five patients (50%) had hypertension, three patients (30%) had diabetes, three patients (30%) had hyperlipidemia, two patients (20%) had coronary heart disease, and one patient (10%) had cerebrovascular disease. None of the nAMD or ARC patients had renal or liver disease. Four patients (40%) and two patients (20%) in the nAMD group compared to three (30%) and four (40%) patients in the ARC group consumed alcohol and smoked, respectively, which were not significant differences. None of the nAMD or ARC patients had polypoidal choroidal vasculopathy or retinal angiomatous proliferation. There were no significant differences in demographics or disease characteristics between the ARC group (controls) and the nAMD group (Table). A color fundus photograph shows newly formed gray-yellow choroidal vessels in an nAMD patient (Fig. 6A). ICGA also showed abnormal neovascularization in the macula in the early stage (Fig. 6B), and fundus fluorescein angiography showed vascular leakage in the late stage for the same nAMD patient (Fig. 6C). Notably, CSF1 (Fig. 6D) and CSF1R (Fig. 6E) protein levels were up-regulated in the AH of CNV patients compared to ARC patients. In summary, our study revealed that under hypoxic conditions, choroidal endothelial cells secreted CSF1. CSF1 bound to CSF1R on the surface of macrophages to activate the PI3K/AKT/FOXO1 pathway and facilitate macrophage migration and M2 polarization. M2-type macrophages enhanced the proliferation, migration, and tube formation of RMECs in a CSF1/CSF1R-dependent manner. CSF1/CSF1R blockade alleviated the formation of mouse laser-induced CNV (Fig. 7).

DISCUSSION

We found that the transcription, expression and secretion of CSF1 were up-regulated in HCVECs after hypoxia. Hypoxia-inducible factor 1 α (HIF-1 α), the principal regulator of hypoxia, is upregulated in choroidal endothelial cells under hypoxia.²¹ The HIF-1 α molecule has two proline (Pro) residues in the 402 and 564 positions. Under normoxia, hydroxylation of the proline residues allows the von-Hippel-Lindau protein to ubiquitinate HIF-1 α , which leads to 26S-dependent proteasomal degradation of the HIF-1 α /HIF-1 β complex. In contrast, under hypoxic conditions, the action of prolyl hydroxylases is blocked,

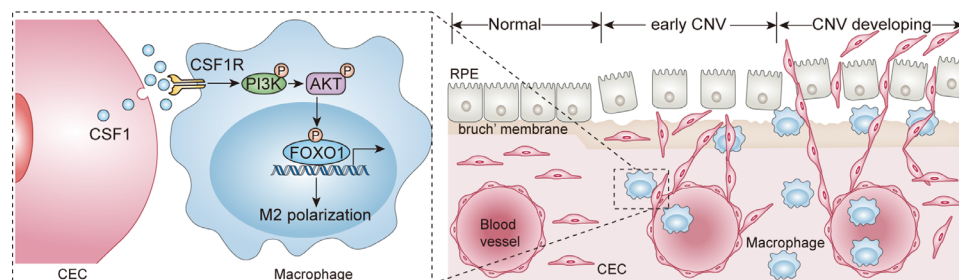


FIGURE 7. Mechanism map was shown. Choroidal vascular endothelial cells (CCECs) release CSF1 under hypoxia. CSF1 binds to CSF1R on macrophages to activate the PI3K/AKT/FOXO1 pathway, which facilitates macrophage migration and M2 polarization. M2-type macrophages enhance the proliferation, migration and tube formation of CCECs in a CSF1/CSF1R-dependent manner to promote the formation of choroidal neovascularization.

and HIF-1 α is phosphorylated, which then binds the cAMP response element binding protein/p300 complex. After HIF-1 β binds HIF-1 α , the HIF-1 α /HIF-1 β dimer binds to the hypoxia response elements of target genes to exert specific effects.²² For example, HIF-1 α mediates CSF1 expression in pancreatic ductal adenocarcinoma cells via direct binding to the hypoxia response element in the CSF-1 promoter.²³ Therefore we hypothesized that HIF-1 α mediated hypoxia-induced CSF-1 expression.

Endothelial-induced macrophages are polarized toward an M2 fate,²⁴ and CSF-1 promotes M2 macrophage polarization.²⁵ When CSF-1 binds to its receptor CSF1R on macrophages, downstream pathways, such as PI3K/AKT and extracellular signal-regulated kinase,²⁶ are activated to initiate macrophage differentiation and polarization. CSF1 facilitated the M2-type polarization of macrophages in the present study via activation of the CSF1R/PI3K/AKT/FOXO1 pathway.

We also found that the blockade of CSF1/CSF1R using a CSF1 neutralizing antibody and the CSF1R inhibitor PLX3397 alleviated the formation of mouse laser-induced CNV. CSF1 monoclonal antibodies and CSF1 inhibitors, including but not limited to PLX3397, were used in clinical trials for multiple inflammatory diseases. For example, randomized controlled dose-ranging trial 2b evaluated the biology, clinical efficacy, and safety of otilimab in patients with rheumatoid arthritis.²⁷ Otilimab acts as a monoclonal antibody that binds to and prevents CSF-1 from connecting with its receptors, and it is being developed for the treatment of rheumatoid arthritis. PLX3397 is the first systemic therapy to show a robust tumor response in tenosynovial giant cell tumors, and it improved patient symptoms and functional outcomes after a randomized phase 3 trial between May 11, 2015, and September 30, 2016.²⁸ PLX3397, also named pexidartinib, is a novel, orally administered small molecule tyrosine kinase inhibitor with strong selective activity against CSF1R.

To confirm the relationship between the CSF1/CSF1R axis and nAMD clinical features, we detected CSF1 and p-CSF1R protein levels in the AH of ARC and nAMD patients. Our results showed that CSF1 and p-CSF1R expression was higher in the AH of nAMD patients than ARC patients. These results suggested that the CSF1/CSF1R axis played a vital role in the pathogenesis of nAMD. A previous study revealed that CSF1 was increased in the iris ciliary body of a rat endotoxin-induced uveitis model, and low-dose lipopolysaccharide pretreatment reduced the expression of CSF1,²⁹ which indicated that CSF1 acted as an inflammatory cytokine in endotoxin-induced uveitis.

Some questions in our study must be investigated in the future, such as the elaboration of the mechanism of CSF1 upregulation in hypoxia-exposed HCVECs and the effect of CSF1 and CSF1R joint inhibition on mouse laser-induced CNV. However, our data showed that HCVECs released more CSF1 under hypoxia. CSF1 binds to CSF1R on macrophages to activate the PI3K/AKT/FOXO1 pathway, which facilitates macrophage migration and M2 polarization. Conversely, M2-type macrophages enhanced the proliferation, migration, and tube formation of HCVECs in a CSF1/CSF1R-dependent manner. Blockade of the CSF1/CSF1R axis mitigated the formation of mouse laser-induced CNV. These data demonstrated the role of the CSF1/CSF1R axis in the formation of CNV and provide potential therapeutic strategies for the treatment of nAMD.

Acknowledgments

Supported by the major project of Nantong city (No. MS22018009), the National Natural Science Foundation of China (No. 82000911), the Jiangsu Provincial Natural Science Foundation Project (No. BK20200209) and the Nantong Commission of Health and Family Planning (No. WKZL2018002). College Student Innovation Program of Nantong University (No. 209).

Disclosure: **Y. Zhou**, None; **J. Zeng**, None; **Y. Tu**, None; **L. Li**, None; **S. Du**, None; **L. Zhu**, None; **X. Cang**, None; **J. Lu**, None; **M. Zhu**, None; **X. Liu**, None

References

- Jaffe GJ, Ciulla TA, Ciardella AP, et al. Dual antagonism of PDGF and VEGF in neovascular age-related macular degeneration: a phase IIB, multicenter, randomized controlled trial. *Ophthalmology*. 2017;124:224–234.
- Jetten N, Verbruggen S, Gijbels MJ, Post MJ, De Winther MP, Donners MM. Anti-inflammatory M2, but not pro-inflammatory M1 macrophages promote angiogenesis in vivo. *Angiogenesis*. 2014;17:109–118.
- He L, Marneros AG. Doxycycline inhibits polarization of macrophages to the proangiogenic M2-type and subsequent neovascularization. *J Biol Chem*. 2012;287:8019–8028.
- Nakamura R, Sene A, Santeford A, et al. IL10-driven STAT3 signalling in senescent macrophages promotes pathological eye angiogenesis. *Nat Commun*. 2015;6:7847.
- Grossniklaus HE, Ling JX, Wallace TM, et al. Macrophage and retinal pigment epithelium expression of angiogenic cytokines in choroidal neovascularization. *Mol Vis*. 2002;8:119–126.
- Hohensinner PJ, Mayer J, Kichbacher J, et al. Alternative activation of human macrophages enhances tissue factor expression and production of extracellular vesicles. *Haematologica*. 2021;106:454–463.
- Manthey CL, Moore BA, Chen Y, et al. The CSF-1-receptor inhibitor, JNJ-40346527 (PRV-6527), reduced inflammatory macrophage recruitment to the intestinal mucosa and suppressed murine T cell mediated colitis. *PLoS One*. 2019;14:e0223918.
- Braza MS, Conde P, Garcia M, et al. Neutrophil derived CSF1 induces macrophage polarization and promotes transplantation tolerance. *Am J Transplant*. 2018;18:1247–1255.
- Alizadeh E, Mammadzadeh P, Andre H. The different facades of retinal and choroidal endothelial cells in response to hypoxia. *Int J Mol Sci*. 2018;19:3846.
- Wang YJ, Zeigler MM, Lam GK, et al. Akt activation regulates macrophage survival and differentiation: role of M-CSF and endogenous ROS. *Blood*. 2005;106:623a–623a.
- Chung S, Kim JY, Song MA, et al. FoxO1 is a critical regulator of M2-like macrophage activation in allergic asthma. *Allergy*. 2019;74:535–548.
- Vergadi E, Ieronymaki E, Lyroni K, Vaporidi K, Tsatsanis C. Akt signaling pathway in macrophage activation and M1/M2 polarization. *J Immunol*. 2017;198:1006–1014.
- Nielsen MC, Andersen MN, Moller HJ. Monocyte isolation techniques significantly impact the phenotype of both isolated monocytes and derived macrophages in vitro. *Immunology*. 2020;159:63–74.
- Krzystolik MG, Afshari MA, Adamis AP, et al. Prevention of experimental choroidal neovascularization with intravitreal anti-vascular endothelial growth factor antibody fragment. *Arch Ophthalmol*. 2002;120:338–346.
- Thylefors B, Chylack LT, Konyama K, et al. A simplified cataract grading system. *Ophthalmic Epidemiol*. 2002;9:83–95.

16. Murga-Zamalloa C, Rolland DCM, Polk A, et al. Colony-Stimulating Factor 1 Receptor (CSF1R) Activates AKT/mTOR Signaling and Promotes T-Cell Lymphoma Viability. *Clin Cancer Res.* 2020;26:690–703.
17. Dong H, Zhang X, Dai X, et al. Lithium ameliorates lipopolysaccharide-induced microglial activation via inhibition of toll-like receptor 4 expression by activating the PI3K/Akt/FoxO1 pathway. *J Neuroinflammation.* 2014;11:140.
18. Lin W, Xu D, Austin CD, et al. Function of CSF1 and IL34 in Macrophage Homeostasis, Inflammation, and Cancer. *Front Immunol.* 2019;10:2019.
19. Perry HM, Okusa MD. Driving change: kidney proximal tubule CSF-1 polarizes macrophages. *Kidney Int.* 2015;88:1219–1221.
20. Xu N, Bo Q, Shao R, et al. Chitinase-3-Like-1 Promotes M2 Macrophage Differentiation and Induces Choroidal Neovascularization in Neovascular Age-Related Macular Degeneration. *Invest Ophthalmol Vis Sci.* 2019;60:4596–4605.
21. Brylla E, Tscheuschilsuren G, Santos AN, Nieber K, Spanel-Borowski K, Aust G. Differences between retinal and choroidal microvascular endothelial cells (MVECs) under normal and hypoxic conditions. *Exp Eye Res.* 2003;77:527–535.
22. Tirpe AA, Gulei D, Ciortea SM, Crivii C, Berindan-Neagoe I. Hypoxia: overview on hypoxia-mediated mechanisms with a focus on the role of HIF genes. *Int J Mol Sci.* 2019;20:6140.
23. Wang H, Jia R, Zhao T, et al. HIF-1 α mediates tumor-nerve interactions through the up-regulation of GM-CSF in pancreatic ductal adenocarcinoma. *Cancer Lett.* 2019;453:10–20.
24. He H, Xu J, Warren CM, et al. Endothelial cells provide an instructive niche for the differentiation and functional polarization of M2-like macrophages. *Blood.* 2012;120:3152–3162.
25. Jones CV, Ricardo SD. Macrophages and CSF-1: implications for development and beyond. *Organogenesis.* 2013;9:249–260.
26. McMahon KA, Wilson NJ, Marks DC, et al. Colony-stimulating factor-1 (CSF-1) receptor-mediated macrophage differentiation in myeloid cells: a role for tyrosine 559-dependent protein phosphatase 2A (PP2A) activity. *Biochem J.* 2001;358:431–436.
27. Kerschbaumer A, Sepriano A, Smolen JS, et al. Efficacy of pharmacological treatment in rheumatoid arthritis: a systematic literature research informing the 2019 update of the EULAR recommendations for management of rheumatoid arthritis. *Ann Rheum Dis.* 2020;79:744–759.
28. Tap WD, Gelderblom H, Palmerini E, et al. Pexidartinib versus placebo for advanced tenosynovial giant cell tumour (ENLIVEN): a randomised phase 3 trial. *Lancet.* 2019;394:478–487.
29. Ling Y, Wang J, Yu S, Li W, Lu H. The protective effect of low dose of lipopolysaccharide pretreatment on endotoxin-induced uveitis in rats is associated with downregulation of CSF-1 and upregulation of LRR-1. *J Immunol Res.* 2020;2020:9314756.